

Cite this article: D. Singh, Green synthesis and characterization of ZnO nanoparticles with leaf extract from *Cayratia pedata*, *RP Cur. Tr. Appl. Sci.* 4 (2025) 6–13.

## Original Research Article

# Green synthesis and characterization of ZnO nanoparticles with leaf extract from *Cayratia pedata*

Devender Singh\*

Department of Physics, Government College, Matanhail (Jhajjar) – 124106, Haryana, India

\*Corresponding author, E-mail: [devender079dudi@gmail.com](mailto:devender079dudi@gmail.com)

### ARTICLE HISTORY

Received: 22 Nov. 2024

Revised: 24 Feb. 2025

Accepted: 27 Feb. 2025

Published: 03 March 2025

### KEYWORDS

Green synthesis;  
Zinc oxide nanoparticles;  
*Cayratia pedata*.

### ABSTRACT

This paper presents a plant-mediated method for synthesizing ZnO nanoparticles. The nitrate derivative of zinc and plant extract from the native medicinal herb *Cayratia pedata* were used to successfully synthesize the nanoparticles. The plant extract was allowed to react with 0.1 mM of Zn (NO<sub>3</sub>)<sub>2</sub>·6H<sub>2</sub>O at several concentrations, while the reaction temperature was kept at 55°C, 65°C, and 75°C. The resulting yellow paste was completely dried, gathered, and sealed for additional examination. An absorption peak peculiar to ZnO nanoparticles was detected at 320 nm in the UV visible spectrometer (UV-Vis). The existence of ZnO nanoparticles in their aggregated form is revealed by the characterization performed with a Field Emission Scanning Electron Microscope (FESEM). The average size of the nanoparticles was calculated to be 52.24 nm based on the X-ray diffraction (XRD) pattern. The composition of zinc and oxygen is revealed by the Energy Dispersive Spectrum (EDX) measurements, which show high energy signals of 78.32% and 12.78% for zinc and oxygen, respectively. Analysis using Fourier Transform-Infra-Red (FT-IR) spectroscopy reveals that the Zn–O bonding absorption peak lies between 400 and 600 cm<sup>-1</sup>. The development of nano ZnO is confirmed by the several characterization techniques used. The enzyme glucose oxidase was immobilized using the produced nanoparticles. When glucose oxidase was immobilized using the green produced ZnO nanoparticles, a relative activity of 60% was achieved. A comparison between native ZnO and the green produced ZnO was also conducted. It was discovered that this green synthesis approach was both economical and environmentally beneficial.

## 1. Introduction

Because of its use in biotechnology, chemistry, and medicine, nanotechnology has grown significantly during the last ten years [1–3]. Advancements in this area have led to new developments in nanoscience, specifically in the areas of drug delivery, gene transport, nanomedicine, biosensing, and more [4, 5]. The high surface-to-volume ratio of nanoparticles is one of their distinctive characteristics that makes them so intriguing [6]. Because atoms on the surface of nanoparticles are often more active than those at the center, this property makes them more reactive than the bulk material [7, 8]. These nanoparticles can be synthesized chemically, physically, or biologically. Numerous physical and chemical techniques, including as lithography, hydrothermal, sol-gel synthesis, and laser ablation, call for specialized tools and trained personnel. They are also harmful to health due to their poisonous effects. The green synthesis process yields nanoparticles that are non-toxic, biodegradable, and reasonably priced [9–12]. Because it uses natural resources like leaves, roots, and flower extracts as well as microorganisms like bacteria, fungi, algae, etc., this environmentally friendly synthesis method uses fewer harmful compounds [13–15].

Recent research demonstrates the importance of environmentally friendly metal oxide nanoparticle synthesis, where metal oxides such as zinc, gold, copper, silver, nickel, and others are becoming more and more significant [16–18]. Our goal is to synthesize nanoparticles that may be used to

create optical biosensors, which prioritizes materials with favorable optical characteristics such as chemiluminescence, photoluminescence, optical absorption, and optical emission [19, 20]. Among the many metal oxides, ZnO nanoparticles have a wide bandgap, good optical transmittance, strong electron mobility, and a substantial exciton binding energy [21, 22]. The development of sensors makes use of ZnO's optical characteristics [23–25].

The plant *Cayratia pedata*, also called the "Birdfoot Grapevine," is a member of the Vitaceae family and is the subject of the current study's green synthesis process for synthesizing ZnO nanoparticles [26]. The southern region of India is home to the native, endangered medicinal plant *Cayratia pedata*. Mostly found in tropical forests, it is a woody climber with a cylindrical stem. The plant's leaf has long been used to cure scabies, inflammation, and ulcers [27]. Alkaloids, tannins, phenolic chemicals, flavonoids, and terpenoids are abundant in the plant extract [28]. The antibacterial [29], anti-ulcer [30], anti-inflammatory [31], anti-arthritis [32], anti-diarrheal [33], anti-oxidant [34], and anti-nociceptive [35] qualities of the plant's crude extracts vary in strength. The synthesis of ZnO nanoparticles from *Cayratia pedata* has never been attempted before. But in the past, *Cayratia pedata* was employed as reducing agent to create silver nanoparticles [36].

Applications for the produced nanoparticles include drug discovery, sensors, lasers, and more. Depending on the



Copyright: © 2025 by the authors. Licensee Research Plateau Publishers, India

This article is an open access article distributed under the terms and conditions of the

Creative Commons Attribution (CC BY) license (<https://creativecommons.org/licenses/by/4.0/>).

application, the synergistic effects can be quantified. Shape and size are crucial in applications that use the anticancer [37], antibacterial [38], antimicrobial [39], antityrosinase [40], and antibiofilm [41] properties of nanoparticles. For instance, spherically shaped ZnO NP is much easier to release Zn<sup>2+</sup> ions than rod-shaped ZnO NP, and tiny particles are more permeable to bacterial membranes [42–44]. Additionally, it has been discovered that ZnO nanoparticles are a superior catalyst that may be regenerated with reduced activity degradation [45]. The characteristics of nanoparticles can be applied in a wide range of fields. However, in order to further improve glucose oxidase as a biosensor, these nanoparticles were specifically produced to encapsulate the enzyme. There have been previous reports of immobilization through the use of the green synthesis approach [46]. However, this is the first study to use green synthesized ZnO nanoparticles to immobilize the glucose-specific enzyme glucose oxidase.

### 1.1 Mechanism of the plant-mediated technique

To transform the metal precursors into metal nanoparticles, the phytochemicals found in the plant extract can function as reducing agents. Because they are toxic-free and antioxidants, phytochemicals can have both lowering and stabilizing effects [47]. Terpenoids, flavonoids, phenolic compounds, aldehydes, and alkaloids are among the vital phytochemicals that have aided in the reduction process. Different plant extracts have varying amounts of these phytochemical lowering agents. Thus, the synthesis of nanoparticles is significantly impacted by the content of the leaf extract. The synthesis, stability, and amount of nanoparticles formed are influenced by variables such pH, temperature, contact time, metal salt concentration, and phytochemical profile of plant extract [48]. In order to stabilize the metal ions following reduction by plant extracts, literature suggested encasing them in an organic covering in three stages.

1. Activation phase: includes nucleation of reduced metal ions and reduction of metal ions,
2. Growth phase: contributes to the stability of nanoparticles,
3. The last stage is comprised of the produced nanoparticles [49].

The activity of phytochemicals causes metals like copper, silver, gold, titanium, zinc, iron, and nickel to create their metal oxides. Metal ions reach the growth and stabilization phase through the action of phytochemicals. Finally, the

joining of metal ions due to oxygen production creates a distinct shape.

Plant extract preparation, mixing the metallic solution with the plant extract, and the creation of biocompatible nanoparticles are the steps in the plant-based extraction mechanism of nanoparticle synthesis. After that, the nanoparticles were characterized using FTIR, SEM, TEM, XRD, and other techniques; the specifics are covered in the next session.

## 2. Materials and methods

### 2.1 Materials

A taxonomist from the Agriculture University, Hisar recognized a fresh *Cayratia pedata* var. *glabra* plant that was obtained from forest of Tamilnadu. Fusion Biotech, New Delhi, supplied the substance utilized in the analysis, zinc nitrate hexahydrate (99.8% purity).

### 2.2 Methods

To get rid of dust and other debris, the plant's leaves are thoroughly cleaned with distilled water. After being cleaned, the plant portion is allowed to air dry at ambient temperature. Fifty grams of leaves were weighed and collected for examination. After being cut into little pieces, they were crushed with a mortar and pestle while enough water was added. To investigate the impact of concentration variation in sample preparation, the extract is made at two distinct concentrations: Sample A (25 gm in 50 ml) and Sample B (25 gm in 100 ml). After 15 minutes of boiling, which weakens the cell membrane, the extract was processed by filtering it through Whatman No. 1 filter paper. After centrifuging it for five minutes at 2400 rpm to get rid of the debris, the supernatant is removed for additional testing.

### 2.3 Green synthesis of nanoparticles

The study uses modified processes from earlier green synthesis work to synthesize ZnO nanoparticles, as shown in Table 1. For the current work, the crucial elements of each of the techniques described here were taken into account. This study attempted to reduce the complexity of the processes performed, the quantity of chemicals employed, and the time required for the analysis without compromising the quality of the synthesized nanoparticle, in contrast to other synthesis procedures where zinc nitrate was considered the precursor.

**Table 1:** Modified methods from other research that served as our study's references.

Sl No.	Plant/fungi/ bacteria (Concentration),	Filtering process/pre heating	Working temperature and condition	References
1	<i>Brassica oleracea</i> L. var. <i>Italic</i> (8g in 80 ml)	At 70°C for 20 min	Heated at 70°C for 20 min + centrifuged at 6000 rpm for 20 min + dried at 80°C for 6 h + calcinated at 450°C	[50]
2	<i>Deverra tortuosa</i> (crude extract of 25 ml)	At 60–80°C	Heated at 60°C overnight + paste collected and heated at 400°C for 2 h	[51]
3	<i>Euphorbia petiolata</i> (50 g in 500 ml)	At 80°C for 30 min	Heated at 80°C for 2 h + centrifuged at 6000 rpm + annealing at 400°C for 2 h	[52]
4	<i>Punica</i>	At 40°C at pH 3 and filtered with Whatman filter paper (0.22 m)	Heated at 80°C + centrifuged at 1000 rpm for 10 min annealing at 400°C and 500°C	[53]
5	<i>Mussaenda frondosa</i> (1:10)	At 100°C for 4 h	Stirring at 450–500 rpm + mix heated at 400°C for 10–30 min in magnetic stirrer	[54]
6	<i>Eucalyptus globulus</i> Labill (20 g in 100 ml)	At 60°C in oven and cooled to room temperature	Centrifuged at 5000 rpm for 1 h + calcined at 400°C for 2 h	[55]

The obtained homogenous leaf extracts were mixed with 5 ml of 10 mM Zn (NO<sub>3</sub>)<sub>2</sub>.6H<sub>2</sub>O and agitated for 20 minutes at 65°C. After turning light yellow, samples A and B were gathered and heated for the entire night at the same temperature until a thick yellow paste was produced. After being fully dried and calcined for two hours at 400°C, this paste was gathered and packaged individually for additional analysis. The process of calcination, which is temperature-dependent, eliminates the contaminants from the sample and yields a pure version of the NP [56]. To finally prove that the sample was ZnO nanoparticles, it was evaluated and measured using a variety of techniques, including UV visible spectrometer, SEM, XRD, EDX, and FT-IR. For temperatures above and below the working temperature, 55°C and 75°C, this process was repeated. Zinc nitrate and plant extract did not react during the experiment at 55°C, which led to the creation of nano ZnO. Furthermore, it produced ashes due to the excessively high temperature of 75°C when employed as the operating temperature. But without any negative effects, a yellow color shift was seen at 65°C. Furthermore, the sample's identity as ZnO nanoparticles was verified during characterization. Therefore, temperature has a significant impact on how nanoparticles form.

## 2.4 Characterization of ZnO nanoparticles

### UV-visible spectroscopy

The absorption spectra of ZnO nanoparticles produced at different temperatures and concentrations were used to observe the optical properties of the nanoparticles. An Ultraviolet-Visible Spectrometer with a wavelength between 200 and 800 nm is used to characterize this. Spectroscopy can also be done using UV light for LEDs. There are three kinds of them. The wavelengths of UV A are 400–315 nm, UV B is 315–280 nm, and UV C is 280–100 nm. The former can be used for generic applications and is more cost-effective, while the latter is more environmentally friendly. Because UV-LEDs are application-specific, we decided to analyze them using UV-visible spectroscopy.

### Scanning electron microscopy

The pictures of the biosynthesized ZnO nanoparticles were captured using a Nova NanoSEM 450 analyzer with an acceleration voltage of 10 KV. The manufactured particles were combined with acetone and allowed to dry on a glass slide to create a thin layer for the analysis before the FESEM images were taken.

X-Ray Diffractogram: The Bruker AXS D8 Advance X-Ray Diffractometer is used to analyze the crystalline material utilizing Cu k-alpha radiation with a wavelength of 1.5402 Å.

### Energy dispersive spectrometry

The composition and elemental data of the nanomaterial were obtained using energy dispersive spectroscopy.

### Fourier transform infrared spectroscopy

The chemical bonds in the manufactured nanoparticles are revealed by the infrared absorption spectra generated by this characterization method. The analysis for this was conducted using the FT-IR Spectrophotometer-Thermo Fisher-Scientific Nicolet iS50. 2.4.5.

### Immobilization of enzymes

The generated nanoparticles were utilized to immobilize the enzyme after being verified as nano ZnO by a variety of

characterization techniques. A straightforward adsorption technique was used to immobilize glucose oxidase on produced ZnO nanoparticles. 1 mg of GO<sub>x</sub> was added to 0.1 M sodium acetate buffer at pH-5 for the adsorption procedure. After adding 0.5 g of ZnO nanoparticles to the aforesaid solution, it was incubated for the entire night at 30°C while being constantly stirred. Other pH values, including 3, 7, and 9, were tested in the experiment. In order to ascertain the amount of enzyme activity upon immobilization, the glucose oxidase activity was measured using the test kit. The assay relied on the enzymatic reaction of immobilized glucose oxidase with the substrate glucose to produce hydrogen peroxide. Colorimetric measurements of the hydrogen peroxide reaction with fluorescent peroxidase substrate are made at 570 nm.

## 3. Results and discussion

### 3.1 UV-visible spectroscopy

Zinc ions in the fluid are reduced to ZnO by secondary metabolites found in plants. In addition to its reducing properties, the plant extract also has stabilizing properties. By analyzing the UV-visible spectrum between 280 and 800 nm, this was verified. The ZnO nanoparticle-specific peak in the spectra was observed at 320 nm. The wavelength range of the absorbance peak for ZnO nanoparticles is reported to be between 310 and 360 nm [57].

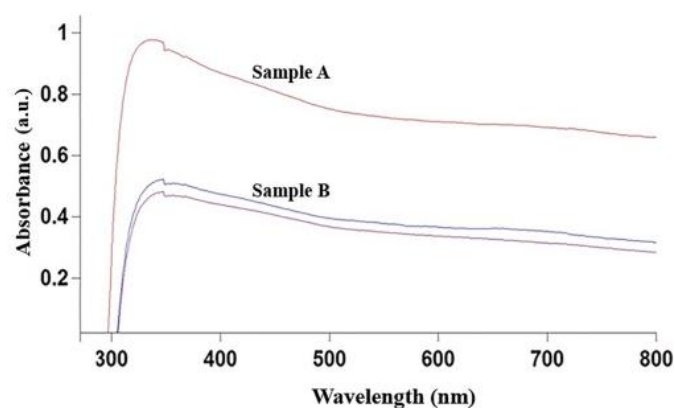


Figure 1: UV-Vis spectra of two distinct concentrations of ZnO nanoparticles.

Because Sample A contains a higher percentage of plant extract, it exhibits greater absorption. Sample B is represented by the graph in Figure 1 that shows a smaller absorption peak. Two absorption peaks are visible in sample B alone. When sample B was first taken for the study, it has a somewhat greater absorption peak. As time progresses, the nanoparticles settle near the bottom of sample B's lowest graph, resulting in a decrease in absorption. Sample A was taken into consideration for additional characterization since it had greater absorbance as a result of its higher concentration. Using  $E_g = 1240/\lambda$  eV, the bandgap energy was computed and found to be 3.8 eV, which is similar to the energy bandgap values for ZnO nanoparticles that have been previously reported [58, 59].

### 3.2 FESEM analysis

As seen in Figure 2, FESEM pictures were captured at various magnifications to investigate the size and form of the synthesized nanoparticles. The agglomerated form of the nanoparticles is confirmed by the surface morphology.

Numerous scholarly works document the impact of surface shape and its correlation with ZnO's synergistic action [60].

The majority of the particles' horizontal shape was discovered, and XRD was used to validate this.

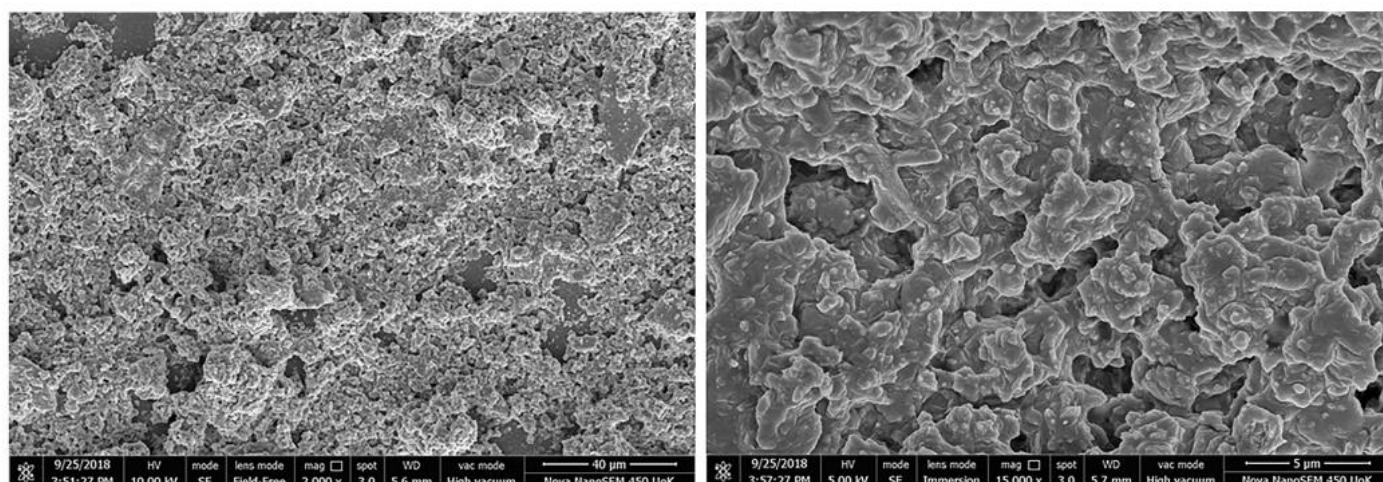


Figure 2: FESEM picture of ZnO nanoparticles at different magnifications.

### 3.3 XRD analysis

The crystalline nature of ZnO nanoparticles is revealed by XRD. The diffractogram displays the diffracted rays' intensity as a function of the diffraction angles. The spectra display the crystal planes' specifics. Table 2 describes the different angles at which the lattice planes (100), (002), (101), (102), and (110) were formed. To determine the nanoparticles' size, the Debye-Scherrer equation was utilized:

$$D = \frac{k\lambda}{\beta \cos \theta} \text{ \AA}$$

where  $k$  is the form factor or Scherrer's constant (0.9),  $\theta$  is Bragg's diffraction angle,  $\beta$  is the XRD peak full width at half maximum,  $D$  is the average crystalline particle size, and  $\lambda$  is the x-ray wavelength (1.5406 Å).

Table 2: Outcomes of XRD study at different angles of diffraction.

Sl. No.	2θ	FWHM (β)	Miller indices	Particle size (D)
1	31.57	0.00229	(100)	60.29
2	34.24	0.00229	(002)	60.29
3	36.07	0.00233	(101)	59.26
4	47.36	0.00243	(102)	56.83
5	56.42	0.00278	(110)	49.74
6	62.69	0.00299	(103)	46.22
7	67.77	0.00325	(112)	42.54
8	68.91	0.00324	(201)	42.70

The average crystallographic size of the synthesized nanoparticles was calculated using Scherrer's formula and was 52.24 nm. The peaks and the ICDD card number 01-079-0207 matched. With lattice parameters  $a (= b)$  equal to 3.2568 Å and  $c$  equal to 5.2125 Å, the nanoparticles were found to have a hexagonal form, which is consistent with values previously reported [61, 62].

### 3.4 EDX analysis

The existence of zinc in the oxide form is confirmed by the high signal for zinc and oxygen that the EDX showed. The EDX provides significant peaks of 78.32% for zinc and

12.78% for oxygen, whose weight percentage peaks are similar to those previously reported for the fabrication of ZnO nanoparticles [63]. This information provides the composition of each element present in the analyte. For zinc, two prominent peaks were found at 1 eV and 8.6 eV, while for oxygen, the signal was visible at 0.5 eV [64, 65]. The elemental makeup of the produced chemical is confirmed by these values, which are particular to zinc and oxygen. Figure 4 illustrates the presence of traces of several chemicals, such as sodium, in addition to zinc and oxygen.

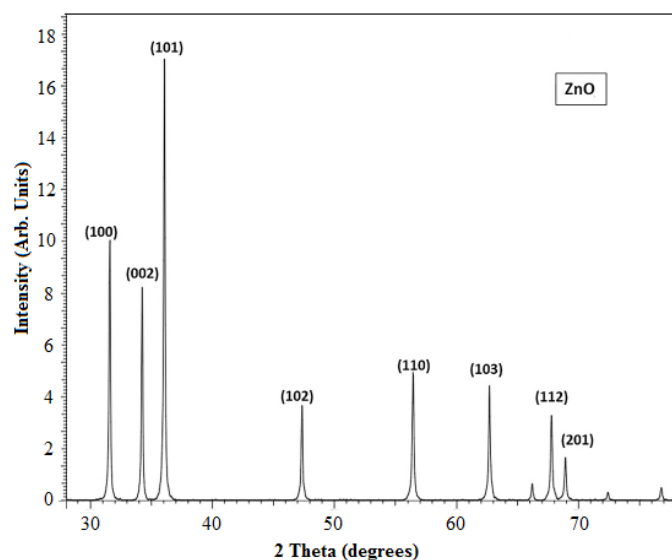


Figure 3: Synthesized ZnO nanoparticles' X-ray diffraction spectrum.

### 3.5 FT-IR analysis

The synthesized ZnO nanoparticles' composition and functional group synthesis are revealed by FT-IR. Additionally, it implies that phenolic chemicals, alkynes, terpenoids, and flavonoids combine to synthesize ZnO nanoparticles. The FT-IR spectra of the synthesized ZnO nanoparticles in the 400–4000  $\text{cm}^{-1}$  range are shown in Figure 5. The reduction of zinc ions to ZnO, which was seen as bands, was caused by the functional groups. Every band represents a different stretching mode.

O-H stretching of phenolic compounds is represented by the wide band seen at  $3275\text{ cm}^{-1}$  [66]. The existence of the alkene group was identified at  $1624\text{ cm}^{-1}$  [67], while the amines' C-N stretching bonds are represented by the band at

$1313\text{ cm}^{-1}$  [68]. The presence of Zn-O stretching bands is responsible for the several sharp bands at  $491\text{ cm}^{-1}$  and  $435\text{ cm}^{-1}$ ; the bands between 1000 and 1300 correlate to the C-O stretching of esters and carboxylic functional groups [69, 70].

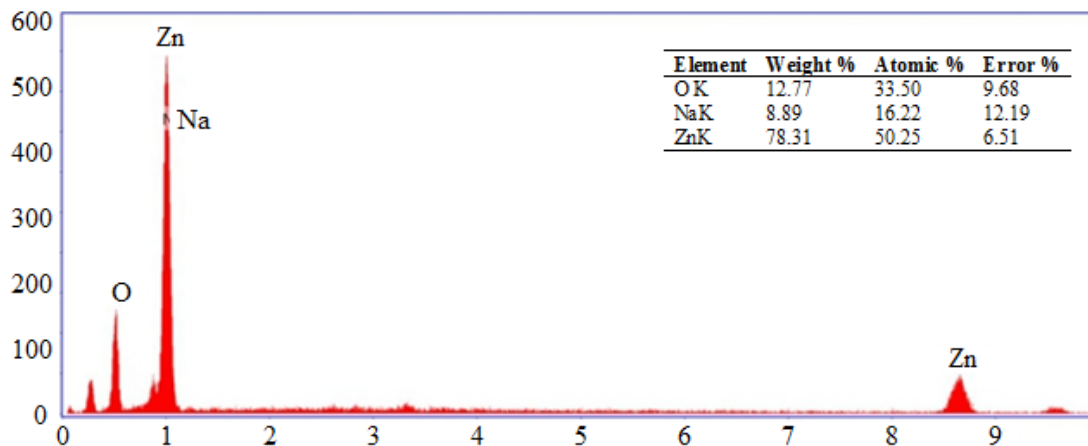


Figure 4: EDX spectrum of synthesized ZnO nanoparticles.

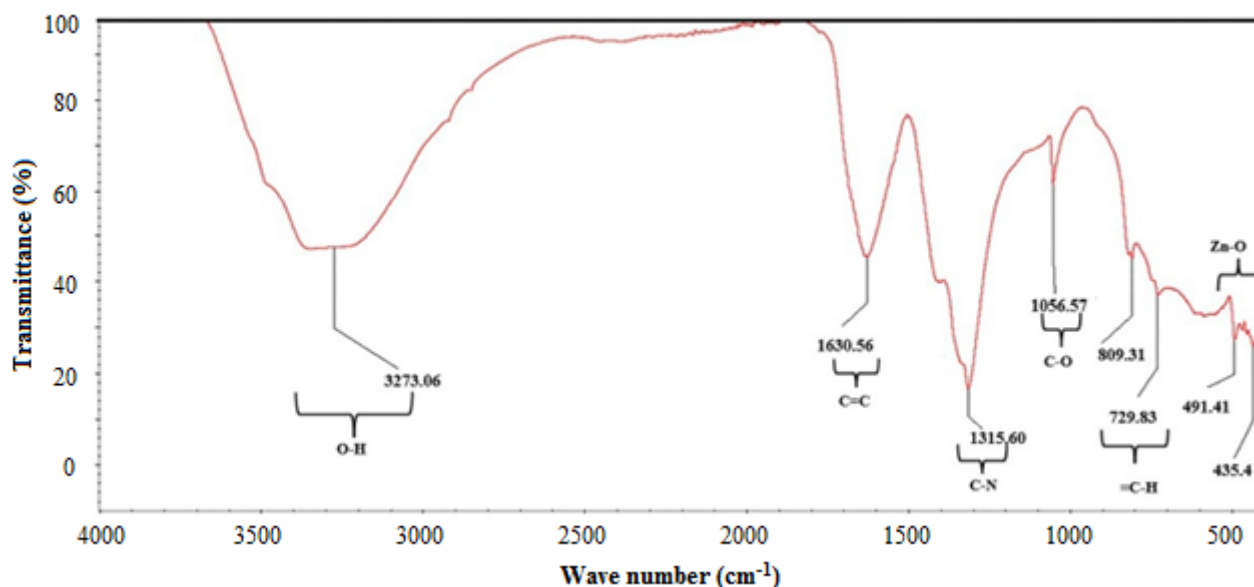


Figure 5: FTIR spectrum of synthesized ZnO nanoparticles.

### 3.6 Immobilization of enzyme

As seen in Figure 6,  $\text{GO}_x$  activity was greater than 50% at all pH levels. At pH 3, the least amount of activity was seen. However, when sodium acetate was utilized as the buffer with green produced ZnO nanoparticles, the maximum activity of roughly 60% was noted at pH 5. After thereafter, there was a minor drop in activity from pH 5 to pH 9. The enzyme activity when adsorbed utilizing native ZnO yielded the highest relative activity of 68% when compared to the relative activity at different pH levels. The enzyme activity previously reported for the immobilization of a cysteine-functionalized enzyme employing ZnO nanoparticles was comparable to this result [71]. In contrast to the green synthesis technique, natural ZnO showed the least activity at pH 7. However, the maximum activity for both ZnO nanoparticles was noted at a pH of 5. This might be expanded to optimize a number of additional parameters, such as concentration, temperature, etc.

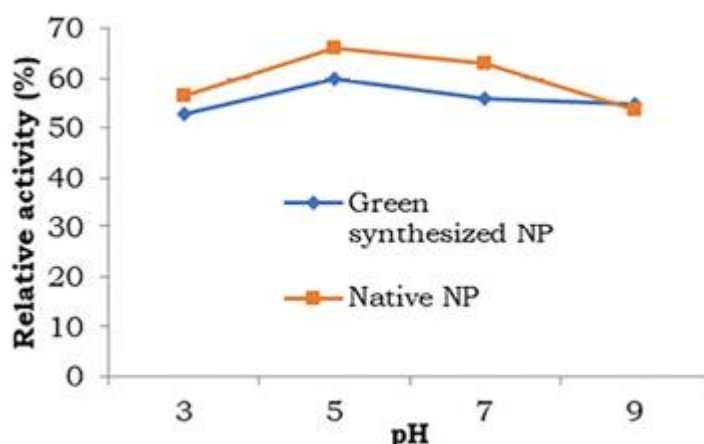


Figure 6: Glucose oxidase's enzyme activity profile employing native and green manufactured nanoparticles at varying pH values.

#### 4. Conclusions

The paper describes a straightforward, economical, and environmentally friendly process for synthesizing ZnO from the plant *Cayratia Pedata* leaf extract. It was discovered that the green synthesis approach, which uses less chemicals to synthesize the nanoparticles, is more environmentally friendly than the traditional methods. Through wet chemical synthesis, nano ZnO of different sizes was produced; the average size was 52.24 nm. The size and structure of ZnO, whose composition and purity were established by EDX tests, are confirmed by SEM analysis. FT-IR spectroscopy was used to analyze the stretching and bonding, while XRD analysis was used to look into the average size and shape of the synthesized nanoparticles. When utilized for enzyme immobilization, the synthesized ZnO nanoparticles provided a relative activity of 60%, or 88.2% of the activity when compared to natural ZnO immobilization.

#### Acknowledgements

The author is very much debited to Dr. S. Duhan, Deenbandhu Chhotu Ram University of Science and Technology, Murthal, India, for providing instrumental facility to carry out the XRD, SEM, EDX and FTIR analyses.

#### Authors' contributions

The author read and approved the final manuscript.

#### Conflicts of interest

The author declares no conflict of interest.

#### Funding

This research received no external funding.

#### Data availability

No new data were created.

#### References

- [1] M. Singh, S. Singh, S. Prasad, I.S. Gambhir, Nanotechnology in medicine and antibacterial effect of silver nanoparticles, *Dig. J. Nanomater. Bios.* **3** (2008) 115–122.
- [2] G.M. Whitesides, Nanoscience, nanotechnology, and chemistry, *Small* **1** (2005) 172–179.
- [3] B. Pelaz, S. Jaber, D.J. De Aberasturi, V. Wulf, T. Aida, J.M. de la Fuente, N. A. Kotov, The state of nanoparticle-based nanoscience and biotechnology: progress, promises, and challenges, *ACS Nano* **6** (2012) 8468–8483.
- [4] C. Jianrong, M. Yuqing, H. Nongyue, W. Xiaohua, L. Sijiao, Nanotechnology and biosensors, *Biotechnol. Adv.* **22** (2004) 505–518.
- [5] X. Zhang, Q. Guo, D. Cui, Recent advances in nanotechnology applied to biosensors, *Sensors* **9** (2009) 1033–1053.
- [6] B.D. Yao, Y.F. Chan, N. Wang, Formation of ZnO nanostructures by a simple way of thermal evaporation, *Appl. Phys. Lett.* **81** (2002) 757–759.
- [7] Y. Yin, R.M. Rioux, C.K. Erdonmez, S. Hughes, G.A. Somorjai, A.P. Alivisatos, Formation of hollow nanocrystals through the nanoscale Kirkendall effect, *Science* **304** (2004) 711–714.
- [8] J.V. Barth, G. Costantini, K. Kern, Engineering atomic and molecular nanostructures at surfaces, in: *Nanoscience and Technology: A Collection of Reviews from Nature Journals*, 2010, pp. 67–75.
- [9] J. Virkutyte, R.S. Varma, Green synthesis of metal nanoparticles: biodegradable polymers and enzymes in stabilization and surface functionalization, *Chem. Sci.* **2** (2011) 837–846.
- [10] M.N. Nadagouda, R.S. Varma, Green synthesis of silver and palladium nanoparticles at room temperature using coffee and tea extract, *Green Chem.* **10** (2008) 859–862.
- [11] M. Darroudi, Z. Sabouri, R.K. Oskuee, A.K. Zak, H. Kargar, M.H.N.A. Hamid, Green chemistry approach for the synthesis of ZnO nanopowders and their cytotoxic effects, *Ceram. Int.* **40** (2014) 4827–4831.
- [12] S. Irvani, Green synthesis of metal nanoparticles using plants, *Green Chem.* **13** (2011) 2638–2650.
- [13] M. Behravan, A.H. Panahi, A. Naghizadeh, M. Ziaee, R. Mahdavi, A. Mirzapour, Facile green synthesis of silver nanoparticles using *Berberis vulgaris* leaf and root aqueous extract and its antibacterial activity, *Int. J. Biol. Macromol.* **124** (2019) 148–154.
- [14] P. Rajiv, S. Rajeshwari, R. Venkatesh, Bio-Fabrication of zinc oxide nanoparticles using leaf extract of *Parthenium hysterophorus* L. and its size-dependent antifungal activity against plant fungal pathogens, *Spectrochim. Acta Mol. Biomol. Spectrosc.* **112** (2013) 384–387.
- [15] G.R. Navale, M. Thiripuranthaka, D.J. Late, S.S. Shinde, Antimicrobial activity of ZnO nanoparticles against pathogenic bacteria and fungi, *JSM Nanotechnol. Nanomed.* **3** (2015) 1033.
- [16] J.S. Moodley, S.B.N. Krishna, K. Pillay, P. Govender, Green synthesis of silver nanoparticles from *Moringa oleifera* leaf extracts and its antimicrobial potential, *Adv. Nat. Sci. Nanosci. Nanotechnol.* **9** (2018), 015011.
- [17] I.M. Chung, A. Abdul Rahuman, S. Marimuthu, A.K. Vishnu Kirthi, P. Anbarasan, Padmini G. Rajakumar, Green synthesis of copper nanoparticles using *Eclipta prostrata* leaves extract and their antioxidant and cytotoxic activities, *Exp. Ther. Med.* **14** (2017) 18–24.
- [18] J. Suresh, G. Pradheesh, V. Alexramani, M. Sundrarajan, S.I. Hong, Green synthesis and characterization of zinc oxide nanoparticle using insulin plant (*Costus pictus* D. Don) and investigation of its antimicrobial as well as anticancer activities, *Adv. Nat. Sci. Nanosci. Nanotechnol.* **9** (2018), 015008.
- [19] C.L. Baird, D.G. Myszka, Current and emerging commercial optical biosensors, *J. Mol. Recogn.* **14** (2001) 261–268.
- [20] J. Shi, Y. Zhu, X. Zhang, W.R. Baeyens, A.M. Garcia-Campana, Recent developments in nanomaterial optical sensors, *Trends Anal. Chem.* **23** (2004) 351–360.
- [21] G. Sangeetha, S. Rajeshwari, R. Venckatesh, Green synthesis of zinc oxide nanoparticles by aloe barbadensis miller leaf extract: structure and optical properties, *Mater. Res. Bull.* **46** (2011) 2560–2566.
- [22] A. Kołodziejczak-Radzimska, T. Jesionowski, Zinc oxide—from synthesis to application: a review, *Materials* **7** (2014) 2833–2881.
- [23] T.V. Kolekar, S.S. Bandgar, S.S. Shirguppikar, V.S. Ganachari, Synthesis and characterization of ZnO nanoparticles for efficient gas sensors, *Arch. Appl. Sci. Res.* **5** (2013) 20–28.
- [24] Z.Q. Zheng, J.D. Yao, B. Wang, G.W. Yang, Light-controlling, flexible and transparent ethanol gas sensor based on ZnO nanoparticles for wearable devices, *Sci. Rep.* **5** (2015) 1107.
- [25] S. Yedurkar, C. Maurya, P. Mahanwar, Biosynthesis of zinc oxide nanoparticles using *ixora coccinea* leaf extract—a green approach, *Open J. Synth. Theor. Appl.* **5** (2016) 1.
- [26] C.P. Khare, *Indian Medicinal Plants- an Illustrated Dictionary*, 1<sup>st</sup> Indian Reprint Springer Pvt. Ltd., New Delhi, India (2007).
- [27] K.S. Manilal, *Vaan Rheede's Hortus Malabaricus with Annotation and Modern Botanical Nomenclature*, Bangalore (2003).
- [28] A.L. Stanley, V.A. Ramani, A. Ramachandran, Phytochemical screening and GC-MS studies on the ethanolic extract of *Cayratia pedata*, *Int. J. Pharm. Phytopharmacol. Res.* **1** (2012) 112–116.

- [29] K. Nayak, J. Lazar, Antimicrobial efficacy of leaf extract of *Cayratia pedata* Lam, Vitaceae. *Int. J. Chemtech. Res.* **6** (2014) 5721–5725.
- [30] P. Karthik, P. Amudha, J. Srikanth, Study on phytochemical profile and antiulcerogenic effect of *Cayratia pedata* Lam in albino wistar rats, *J. Pharmacol. (Paris)* **2** (2010) 1017–1029.
- [31] V. Rajendran, V. Rathinambal, V. Gopal, A preliminary study on anti-inflammatory activity of *Cayratia pedata* leaves on Wister albino rats, *Der. Pharmacia. Lett.* **3** (2011) 433–437.
- [32] K. Selvarani, G.V.S. Bai, Anti-arthritis activity of *Cayratia pedata* leaf extract in Freund's adjuvant induced arthritic rats, *Int. J. Res. Pharm. Sci.* **4** (2014) 55–59.
- [33] P. Karthik, R.N. Kumar, P. Amudha, Anti-diarrheal activity of the chloroform extract of *Cayratia pedata* Lam in albino wistar rats, *J. Pharmacol. (Paris)* **2** (2011) 69–75.
- [34] C. Rice-Evans, N. Miller, G. Paganga, Antioxidant properties of phenolic compounds, *Trends Plant. Sci.* **2** (1997) 152–159.
- [35] V. Rajendran, S. Indumathy, V. Gopal, Anti-nociceptive activity of *Cayratia pedata* in experimental animal models, *J. Pharm. Res.* **4** (2011) 852–853.
- [36] V. Subramani, J.J. Jeyakumar, M. Kamaraj, B. Ramachandran, Plant extracts derived silver nanoparticles, *Int. J. Pharmaceut. Sci. Rev. Res.* **3** (2014) 16–19.
- [37] M.D. Jayappa, C.K. Ramaiah, M.A.P. Kumar, D. Suresh, A. Prabhu, R.P. Devasya, S. Sheikh, Green synthesis of zinc oxide nanoparticles from the leaf, stem and in vitro grown callus of *Mussaenda frondosa* L.: characterization and their applications, *Appl. Nanosci.* **10** (2020) 3057–3074.
- [38] M. Naseer, U. Aslam, B. Khalid, B. Chen, Green route to synthesize Zinc Oxide Nanoparticles using leaf extracts of *Cassia fistula* and *Melia azadarach* and their antibacterial potential, *Sci. Rep.* **10** (2020) 1–10.
- [39] N. Supraja, T.N.V.K.V. Prasad, A.D. Gandhi, D. Anbumani, P. Kavitha, R. Babujanarthanam, Synthesis, characterization and evaluation of antimicrobial efficacy and brine shrimp lethality assay of *Alstonia scholaris* stem bark extract mediated ZnONPs, *Biochem. Biophys. Rep.* **14** (2018) 69–77.
- [40] M. Darroudi, S. Ranjbar, M. Esfandiari, M. Khoshneviszadeh, M. Hamzehloueian, M. Khoshneviszadeh, Y. Sarrafi, Synthesis of novel triazole incorporated thiazolone motifs having promising antityrosinase activity through green nanocatalyst Cu- $\text{Fe}_3\text{O}_4/\text{SiO}_2$  (TMS-EDTA), *Appl. Organomet. Chem.* **34** (2020), e5962.
- [41] P.P. Mahamuni, P.M. Patil, M.J. Dhanavade, M.V. Badiger, P.G. Shadija, A. C. Lokhande, R.A. Bohara, Synthesis and characterization of zinc oxide nanoparticles by using polyol chemistry for their antimicrobial and antibiofilm activity, *Biochem. Biophys. Rep.* **17** (2019) 71–80.
- [42] S. Alamdari, M. Sasani Ghamsari, C. Lee, W. Han, H.H. Park, M.J. Tafreshi, H. Afarideh, M.H.M. Ara, Preparation and characterization of zinc oxide nanoparticles using leaf extract of *Sambucus ebulus*, *Appl. Sci.* **10** (2020) 3620.
- [43] Y.H. Leung, C.M.N. Chan, A.M.C. Ng, H.T. Chan, M.W.L. Chiang, Antibacterial activity of ZnO nanoparticles with a modified surface under ambient illumination, *Nanotechnology* **23** (2012) 475703.
- [44] M. Arakha, M. Saleem, B.C. Mallick, S. Jha, The effects of interfacial potential on antimicrobial propensity of ZnO nanoparticles, *Sci. Rep.* **5** (2015) 9578.
- [45] K.V.V. Satyanarayana, P.A. Ramaiah, Y.L.N. Murty, M.R. Chandra, S.V.N. Pammi, Recyclable ZnO nano particles: economical and green catalyst for the synthesis of  $\text{A}_3$  coupling of propargylamines under solvent free conditions, *Catal. Commun.* **25** (2012) 50–53.
- [46] M. Švecov' a, O. Volochanskyi, M. Dendisov' a, D. Palounek, P. Mat' ejka, Immobilization of green-synthesized silver nanoparticles for micro- and nano-spectroscopic applications: what is the role of used short amino- and thio-linkers and immobilization procedure on the SERS spectra? *Spectrochim. Acta Mol. Biomol. Spectrosc.* **247** (2021) 119142.
- [47] J. Singh, T. Dutta, K.H. Kim, M. Rawat, P. Samddar, P. Kumar, 'Green' synthesis of metals and their oxide nanoparticles: applications for environmental remediation, *J. Nanobiotechnol.* **16** (2018) 1–24.
- [48] K.S. Mukunthan, S. Balaji, Cashew apple juice (*Anacardium occidentale* L.) speeds up the synthesis of silver nanoparticles, *Int. J. Green Nanotechnol.* **4** (2012) 71–79.
- [49] A.J. Love, V.V. Makarov, O.V. Sinityna, J. Shaw, I.V. Yaminsky, N.O. Kalinina, M. A. Taliansky, Genetically modified tobacco mosaic virus that can produce gold nanoparticles from a metal salt precursor, *Front. Plant Sci.* **6** (2015) 984.
- [50] J. Osuntokun, D.C. Onwudiwe, E.E. Ebenso, Green synthesis of ZnO nanoparticles using aqueous *Brassica oleracea* L. var. *italica* and the photocatalytic activity, *Green Chem. Lett. Rev.* **12** (2019) 444–457.
- [51] M. Aminuzzaman, L.P. Ying, W.S. Goh, A. Watanabe, Green synthesis of zinc oxide nanoparticles using aqueous extract of *Garcinia mangostana* fruit pericarp and their photocatalytic activity, *Bull. Mater. Sci.* **41** (2018) 50.
- [52] C. Mohammadi, S. Mahmud, S.M. Abdullah, Y. Mirzaei, Green synthesis of ZnO nanoparticles using the aqueous extract of *Euphorbia petiolata* and study of its stability and antibacterial properties, *Moroc. J. Chem.* **5** (2017) 5–13.
- [53] X. Fuku, A. Diallo, M. Maaza, Nanoscaled electrocatalytic optically modulated ZnO nanoparticles through green process of *Punica granatum* L. and their antibacterial activities, *Int. J. Electrochem.* (2016).
- [54] M.D. Jayappa, C.K. Ramaiah, M.A.P. Kumar, D. Suresh, A. Prabhu, R.P. Devasya, S. Sheikh, Green synthesis of zinc oxide nanoparticles from the leaf, stem and in vitro grown callus of *Mussaenda frondosa* L.: characterization and their applications, *Appl. Nanosci.* (2020) 1–18.
- [55] A.A. Barzinjy, H.H. Azeez, Green synthesis and characterization of zinc oxide nanoparticles using *Eucalyptus globulus* Labill. leaf extract and zinc nitrate hexahydrate salt, *SN Appl. Sci.* **2** (2020) 1–14.
- [56] R. Nayak, Ali, D.K. Mishra, D. Ray, V.K. Aswal, S.K. Sahoo, B. Nanda, Fabrication of CuO nanoparticle: an efficient catalyst utilized for sensing and degradation of phenol, *J. Mater. Res.* **9** (2020) 11045–11059.
- [57] M. Sasani Ghamsari, S. Alamdari, W. Han, H. Park, Impact of nanostructured thin ZnO film in ultraviolet protection, *Int. J. Nanomed.* **12** (2016) 207–216.
- [58] S.T. Tan, B.J. Chen, X.W. Sun, W.J. Fan, H.S. Kwok, X.H. Zhang, S.J. Chua, Blueshift of optical band gap in ZnO thin films grown by metal-organic chemical-vapor deposition, *J. Appl. Phys.* **98** (2005), 013505.
- [59] M.K. Debanath, S. Karmakar, Study of blueshift of optical band gap in zinc oxide (ZnO) nanoparticles prepared by low-temperature wet chemical method, *Mater. Lett.* **111** (2013) 116–119.
- [60] X. Peng, S. Palma, N.S. Fisher, S.S. Wong, Effect of morphology of ZnO nanostructures on their toxicity to marine algae, *Aquat. Toxicol.* **102** (2011) 186–196.
- [61] S.T. Fardood, A. Ramazani, S. Moradi, P.A. Asiabi, Green synthesis of zinc oxide nanoparticles using Arabic gum and photocatalytic degradation of direct blue 129 dye under visible light, *J. Mater. Sci. Mater. Electron.* **28** (2017) 13596–13601.
- [62] R. Vinayagam, R. Selvaraj, P. Arivalagan, T. Varadavenkatesan, Synthesis, characterization and photocatalytic dye degradation capability of *Calliandra haematocephala*-mediated zinc oxide

- nanoflowers, *J. Photochem. Photobiol. B Biol.* **203** (2020) 111760.
- [63] S. Pai, H. Sridevi, T. Varadavenkatesan, R. Vinayagam, R. Selvaraj, Photocatalytic zinc oxide nanoparticles synthesis using *Peltophorum pterocarpum* leaf extract and their characterization, *Optik* **185** (2019) 248–255.
- [64] W.N. Unertl, J.M. Blakely, Growth and properties of oxide films on Zn (0001), *Surf. Sci.* **69** (1977) 23–52.
- [65] S. Fakhari, M. Jamzad, H. Kabiri Fard, Green synthesis of zinc oxide nanoparticles: a comparison, *Green Chem. Lett. Rev.* **12** (2019) 19–24.
- [66] M. Ganesh, S.G. Lee, J. Jayaprakash, M. Mohankumar, H.T. Jang, *Hydnocarpus alpina* Wt extract mediated green synthesis of ZnO nanoparticle and screening of its anti-microbial, free radical scavenging, and photocatalytic activity, *Biocatal. Agric. Biotechnol.* **19** (2019) 101129.
- [67] D. Hu, W. Si, W. Qin, J. Jiao, X. Li, X. Gu, Y. Hao, Cucurbita pepo leaf extract induced synthesis of zinc oxide nanoparticles, characterization for the treatment of femoral fracture, *J. Photochem. Photobiol. B Biol.* **195** (2019) 12–16.
- [68] K.D. Sirdeshpande, A. Sridhar, K.M. Cholkar, R. Selvaraj, Structural characterization of mesoporous magnetite nanoparticles synthesized using the leaf extract of *Calliandra haematocephala* and their photocatalytic degradation of malachite green dye, *Appl. Nanosci.* **8** (2018) 675–683.
- [69] C. Chen, B. Yu, P. Liu, J. Liu, L. Wang, Investigation of nano-sized ZnO particles fabricated by various synthesis routes, *J. Ceram. Process. Res.* **12** (2011) 420–425.
- [70] J. Lu, I. Batjikh, J. Hurh, Y. Han, H. Ali, R. Mathiyalagan, D.C. Yang, Photocatalytic degradation of methylene blue using biosynthesized zinc oxide nanoparticles from bark extract of *Kalopanax septemlobus*, *Optik* **182** (2019) 980–985.
- [71] N. Verma, N. Kumar, L.S.B. Upadhyay, R. Sahu, A. Dutt, Fabrication and characterization of cysteine-functionalized zinc oxide nanoparticles for enzyme immobilization, *Anal. Lett.* **50** (11) (2017) 1839–1850.